JOURNAL OF CATALYSIS 75, 275–283 (1982)

Transient Infrared Studies of Carbon Monoxide Oxidation on a Supported Platinum Catalyst

S. M. DWYER

Exxon Chemical Company, Plastics Technology Division, P. O. Box 4255, Baytown, Texas 77520

AND

C. O. BENNETT

The University of Connecticut, Storrs, Connecticut 06268

Received June 22, 1981; revised December 17, 1981

The oxidation of carbon monoxide on a 9.1 wt% Pt/silica catalyst was studied by infrared spectroscopy using the transient method. The technique involved sending step functions in concentration to an infrared cell while the surface coverage of CO was continuously monitored. In the temperature range, 100°C $\leq T \leq$ 160°C, O_2(g) reacted with preadsorbed carbon monoxide via the Langmuir–Hinshelwood (LH) mechanism. This reaction was characterized by an induction period which was dependent upon the temperature and the residence time of CO(g) in the reactor. When CO(g) reacted with preadsorbed oxygen in the same temperature range, the reaction proceeded initially via the modified Eley–Rideal (MER) process. As CO accumulated on the surface of the catalyst, the controlling mechanism shifted from the MER to the LH. The desorption of CO was also observed on this catalyst. For temperatures below 100°C, CO was irreversibly adsorbed. Between 100 and 160°C, a weakly bonded CO species desorbed with an activation energy of 8 kcal/mole.

1. INTRODUCTION

A powerful means of studying the mechanisms of catalytic reactions involves the use of transient methods. These methods, which have become popular over the last 10 years (*1*), are based on the introduction of a step change in feed composition or flow rate to a well-defined isothermal reactor. The outlet concentration is then continuously monitored by a mass spectrometer. From the measured response of the concentration in the reactor, one is able to calculate kinetic parameters for a possible sequence of elementary steps. The advantage of this type of transient experiment over a steady-state experiment is that a larger amount of information is produced concerning the kinetics of a sequence of steps.

Even more direct information on the sequence of steps can be obtained if the surface composition can be followed as it responds to perturbations. Infrared spectroscopy is one of the few techniques which can be used for *in situ* experiments in atmospheric pressure, or above. However, only a few systems meet all the requirements for such experiments.

We chose to study the oxidation of carbon monoxide on a Pt/silica catalyst. Some reasons for choosing this reaction were because the adsorbed intermediate, CO, could be measured easily by its intense absorption band (*2*), the Pt/silica catalyst has good transmission properties for infrared spectroscopy (3), and previous work with this reaction has already been done by other investigators in this laboratory (*4*). Also, as outlined below, there still are some disagreements about the reaction mechanism, and IR transient experiments should help resolve these.

In general, investigators agree that the following steps represent the most probable

0021-9517/82/060275-09$02.00/0

reactions involved in the oxidation of carbon monoxide:

$$CO + * \rightleftharpoons CO^{\bullet} * \quad 1$$

$$O_2 + 2* \longrightarrow 2O^{\bullet\bullet} \quad 2$$

$$CO + O^{\bullet\bullet} \longrightarrow CO_2 + * \quad 3$$

$$CO^{\bullet\bullet} + O^{\bullet\bullet} \longrightarrow CO_2 + 2* \quad 4$$

where step 1 represents the adsorption/desorption of carbon monoxide, step 2 the adsorption of O_2, step 3 the Eley–Rideal (ER) step, and step 4 the Langmuir–Hinshelwood (LH) step. The adsorption and desorption of CO and the adsorption of O_2 have been widely accepted by investigators as important steps in the oxidation of CO. Steps 3 and 4, however, have been the subject of much controversy.

From the literature, it appears that the LH mechanism is dominant at high CO surface coverages and low temperatures (*5, 6*), while the ER mechanism is dominant at low CO surface coverages and high temperatures (*7, 8*). By studying surface transients of adsorbed carbon monoxide, we have gained significant insight regarding which mechanism, LH and ER, is the dominant one at temperatures below 160°C.

2. EXPERIMENTAL METHODS

2.1. Sample Preparation

The catalyst was prepared by pressing 6.41 mg of 9.1 wt% Pt/silica powder on a 1-cm-diameter stainless-steel mirror. The pellet was loaded into a sample cell and reduced *in situ* with flowing H_2 at 250°C. The catalyst powder was prepared by slurrying nonporous silica with an aqueous solution of chloroplatinic acid, followed by air drying in an oven at 100°C. Prior to each transient run, the catalyst surface was cleaned *in situ* by heating the sample cell to 175°C for 1½ h with 3% O_2 in Argon flowing through the reactor.

The particle size of the Pt metal on the support was measured by using transmission electron microscopy. From direct measurement of the micrographs, the results indicated that the crystallite size ranges from 66 to 390 Å. The averaged particle size was calculated to be 200 Å (based on 30 random measurements).

2.2. Reactor Cell

The optical design of the infrared spectrometer used for this study has been previously reported by Ueno *et al.* (*9*). The infrared cell employed (Fig. 1) was made of stainless steel with an Irtran 6 CdTe window. The window, which was transparent in the spectral region of 4000 to 400 cm^{-1}, was glued to the cover by Vacseal cement at an angle of approximately 12° to the mirror so that the reflection from the window would not confound the signal. Because the Vacseal cement softens at approximately 350°C, the reactor was limited to temperatures below this value. The stainless-steel cover was sealed against the main structure of the reactor by a gold gasket. The catalyst pellet, held to the stainless-steel mirror by a sample holder, was positioned in the reactor so that the infrared beam passed through the middle. As shown in Fig. 1, gases entered and left the reactor chamber via 1/16-in.-diameter openings. The reactor volume was 1.1 ml. The pellet thicknesses used were of the order of 5 mg/cm^2. A simple calculation shows that the inner side of the disk would respond by diffusion to a step function of concentration in the gas to within 99% of its final value within less than 1 s. This time is below the resolving power of our experiments.

The metal mirror and sample holder were in direct contact with the main body of the cell which was heated by heating tape wrapped around the outside. The tempera-

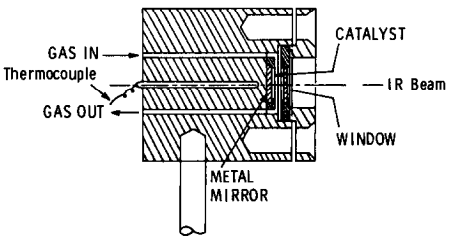

FIG. 1. Reactor schematic.

ture of the catalyst pellet was measured by an iron–constantan thermocouple located immediately behind the metal mirror.

2.3. *Flow System*

The flow system for this study was designed so that the reactor could be subjected to a step change in composition or flow rate. Instantaneous switches between two feed streams was accomplished by locating a Carle Valve (a chromatographic-type four-way valve) upstream from the reactor. Restriction valves located downstream of the reactor were carefully adjusted so that switches between feed streams did not change the flow rate or create appreciable pressure disturbances in the reactor.

Standard 1/8-in. copper tubing was employed throughout the flow system except for short 1/16-in. stainless-steel segments connected to the Carle valves and the reactors. The tubing was connected by Swagelok fittings. Details of a similar flow system are given in a review article (*10*).

2.4. *Chemicals*

The gas mixtures employed for this study were prepared in this laboratory according to the standard procedure previously reported by Cutlip (*4*). Pure gases for the mixture, obtained from Matheson, were passed through desiccant driers before being used.

3. RESULTS

A typical spectrum of carbon monoxide adsorbed on the 9.1 wt% Pt/silica catalyst is shown in Fig. 2. The catalyst was cleaned in 3% O_2/Ar at 175°C. Then the spectrum was recorded while 2% CO/Ar at 100°C was flowing through the reactor. The frequency of the absorption band was dependent on temperature with a maximum frequency of 2080 cm^{-1} at 100°C and a minimum frequency of 2074 cm^{-1} at 160°C. The band half-width (v = 25 cm^{-1}) and extinction coefficient of the absorption band were independent of temperature between 100 and 160°C. No bridge CO at 1850 cm^{-1} was observed, in agreement with previous investigators for Pt/SiO_2 catalysts (*2*, *3*).

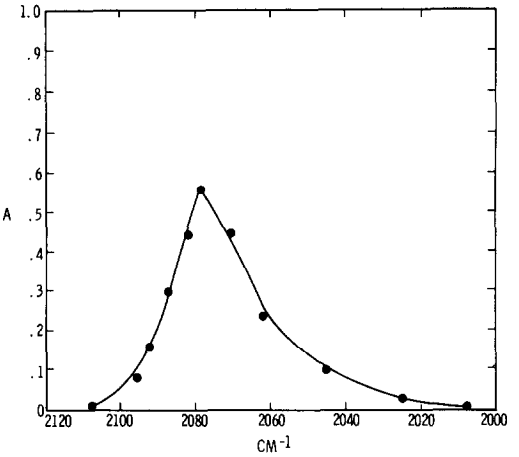

FIG. 2. Typical spectrum of adsorbed CO at 100°C.

3.1. *Desorption Experiments*

The desorption of carbon monoxide from the Pt/silica catalyst was measured by first flowing a 2% CO/Ar mixture over the catalyst until the surface was saturated. Then at t = 0, the feed stream was switched to pure helium which had a flow rate of 130 cm^3/min (reactor temperature and pressure). The helium stream was purified by a Matheson Hydroxy purifier in order to maintain the oxygen concentration below approximately 0.1 ppm. With helium flowing through the reactor, a spectrum of CO was recorded recurrently on a X − Y recorder.

The decreases observed in the intensities of the CO band after the feed stream was switched from 2% CO/Ar to pure He (t = 0) are shown in Fig. 3, where the intensities relative to their saturation values are plotted against time. Assuming that the extinction coefficient of CO adsorbed on Pt is independent of surface coverage at high coverages (*2*), the values of A/As are equal to the fractional surface coverage of CO. Figure 3 shows that for 100°C ≤ T ≤ 160°C, a small fraction of the carbon monoxide was reversibly adsorbed. For temperatures be-

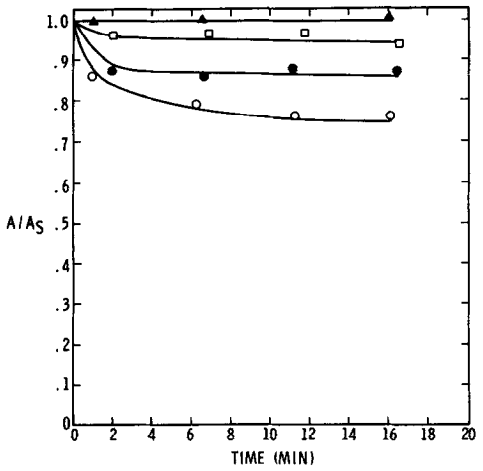

FIG. 3. Rate of CO desorption. (▲) 100°C, (□) 120°C, (●) 140°C, (○) 160°C.

low 100°C, CO was entirely irreversibly adsorbed.

The activation energy for the weakly bonded CO was calculated by assuming the desorption of CO obeys first order kinetics (*11*). Since the residence time of helium in the reactor was approximately 0.51 s, readsorption of carbon monoxide was neglected. At each temperature, slopes of the curves in Fig. 3 were calculated graphically for various fractional surface coverages of carbon monoxide. The results are shown in Fig. 4. As expected, the rate of desorption is first order with respect to the fractional surface coverage of CO. From these results, the activation energy was calculated to be 8 kcal/mole.

3.2. Surface CO during Transient Experiments

The variation in the surface coverage of CO when CO(g) reacts with preadsorbed O and when O_2(g) reacts with preadsorbed CO was observed by periodically switching between feed streams with mixtures of 2% CO and 3% O_2 in argon while monitoring the CO(v). Enough time was allowed between each switching so that the surface was saturated with the gas flowing at that moment. Transient runs were conducted at 100, 120, 140, and 160°C and at various flow rates. Typical transient curves obtained from these switchings are shown in Figs. 5 and 6, respectively. The fractional surface coverage was calculated from the data by assuming the peak height was proportional to the peak area and the position of the band maximum remained constant as the oxidation proceeded. The inherent lag times for the system were taken into account for each of the curves.

3.2.1. Reaction of CO(g) with preadsorbed oxygen. The results from these transient runs indicate that the adsorption of carbon monoxide within experimental error was independent of flow rate for constant temperatures. Figure 6 shows the adsorp-

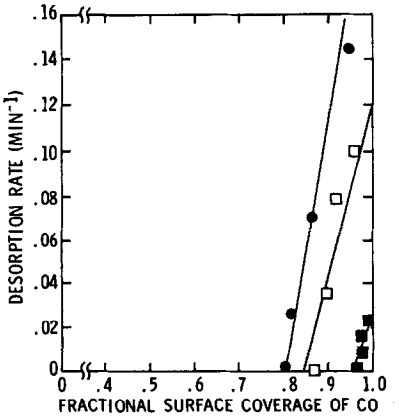

FIG. 4. Rate of desorption of CO as a function of the fractional surface coverage of CO. (●) 160°C, (□) 140°C, (■) 120°C.

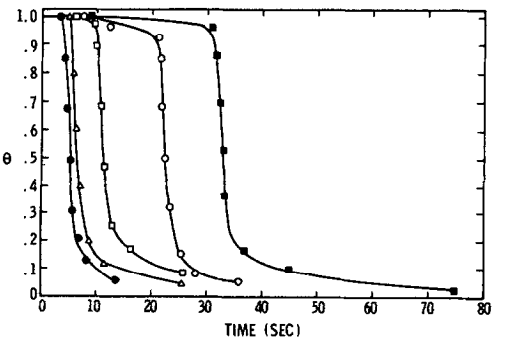

FIG. 5. Reaction between O_2(g) and preadsorbed CO. T = 120°C, (■) 9.5 cm³/min, (○) 18 cm³/min, (□) 57 cm³/min, (▲) 114 cm³/min, (●) 133 cm³/min. Flow rates are at reactor temperature and pressure.

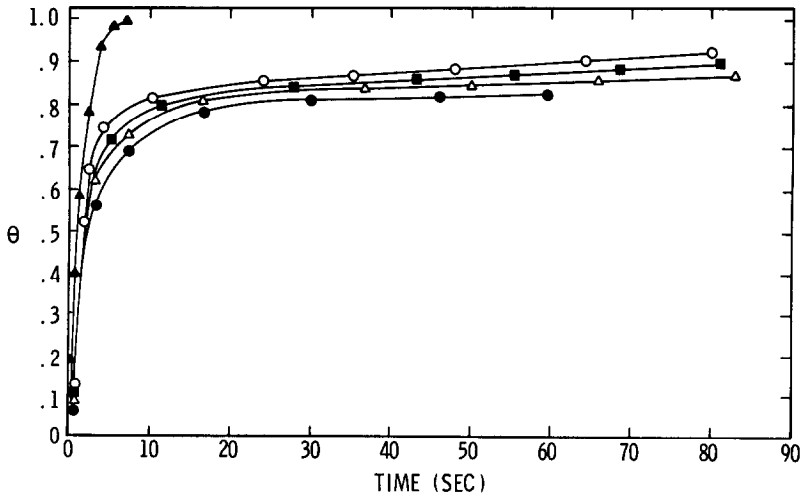

FIG. 6. Reaction between CO(g) and preadsorbed O as a function of temperature. (●) 100°C, (△) 120°C, (■) 140°C, (○) 160°C, (▲) response time of the system.

tion of CO as a function of temperature. Initially the rate of adsorption of CO was very rapid and independent of temperature and then decreased and became temperature dependent. The response time of the system is also included with the adsorption curves. We see that the response time of the system (τ = 1.36 s) is much faster than the adsorption period of CO.

At the slower flow rates, 9.5 and 20 cm³/min, the formation of CO_2 was detectable be monitoring the wavenumber corresponding to the R branch of the gas-phase spectrum of CO_2. The results showed that for all temperatures, CO_2 was evolved at the same time carbon monoxide started to adsorb rapidly on the catalyst surface. A typical result is shown in Fig. 7.

3.2.2. Reaction of $O_2(g)$ with preadsorbed CO. As indicated in Fig. 5, the results of these transient runs showed there was an "induction period" before adsorbed CO reacted with gas phase oxygen. The induction period was measured from when the feed stream was switched from 2% CO/Ar to 3% O_2/Ar, t = 0, to the beginning of the precipitous portion of the transient curve, subtracting out the appropriate inherent lag time of the flow rate used. The effect of temperature and flow rate on the induction time is shown in Fig. 8 where

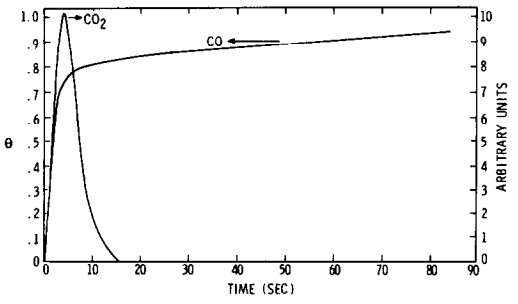

FIG. 7. Typical results for the reaction between CO and preadsorbed 0. T = 160°C, Flow rate = 9.5 cm³/min (160°C).

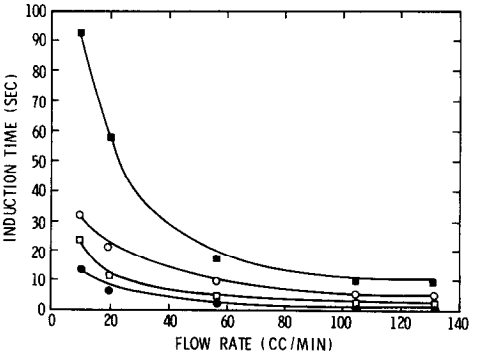

FIG. 8. The effect of flow rate and temperature on the induction period. (■) 100°C, (○) 120°C, (□) 140°C, (●) 160°C.

induction time is plotted against flow rate for constant temperatures. As the temperature decreased the curves became more parabolic suggesting that the effect of flow rate on the induction time is more important at the lower temperatures.

The formation of CO_2, as in the previous transient runs, was observed by monitoring the CO_2(v). The results showed that for each temperature CO_2 was evolved at the same time the surface coverage underwent a rapid change. A typical result is given in Fig. 9.

3.3. Surface Coverages of Adsorbed O and CO

The amount of adsorbed O and CO on the Pt/silica catalyst was calculated at 100, 120, 140, and 160°C by using the reaction of CO(g) with preadsorbed O and O_2(g) with preadsorbed CO. The amount of CO_2 produced from these reactions was proportional to the amount of the adsorbed species.

The procedure was similar to the procedure employed in the previous section. A short helium flush between the switches in the feed stream and slower flow rates (~2.1 cm³/min), however, were used to ensure that there would be no gas phase reaction and to increase the conversion for these reactions.

In order to analyze the resulting transient

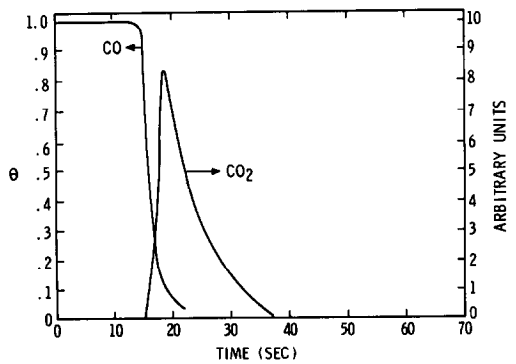

FIG. 9. Typical results for the reaction between O_2(g) with preadsorbed CO. T = 160°C, flow rate = 9.5 cm³/min (160°C).

TABLE 1

Saturation Coverages of CO and Oxygen

Temperature (°C)	Surface coverage of oxygen (molec/g_{cat})	Surface coverage of CO (molec/g_{cat})	Surface coverage of CO_{corr} (molec/g_{cat})
100	1.29×10^{19}	1.15×10^{19}	1.15×10^{19}
120	1.32×10^{19}	1.23×10^{19}	1.30×10^{19}
140	1.41×10^{19}	1.24×10^{19}	1.42×10^{19}
160	1.56×10^{19}	1.26×10^{19}	1.63×10^{19}

CO_2 peaks quantitatively, the spectrometer was calibrated at each temperature by recording a spectrum of the gas phase CO_2 band when known gas mixtures of CO_2 were fed to the reactor. For this study, 2% CO_2 (in Ar) and 1% CO_2 (in Ar) were employed as standards. From the results, a calibration curve was constructed at each temperature where the peak heights of the CO_2 bands were plotted against their respective concentration.

Column 1 and 2 in Table 1 list the amounts of adsorbed O and CO per gram of catalyst for the various temperatures. The saturation values of CO in Column 2, however, had to be corrected for the CO which desorbed during the He flush. The amount of CO was calculated from the desorption curves in Fig. 5. Column 3 lists the new saturation values. Because oxygen does not desorb in this temperature range (*12*), corrections to its saturation values were not necessary.

4. DISCUSSION OF RESULTS

4.1. Desorption Experiments

The activation energy of desorption of CO from Pt has usually been measured under conditions of relatively low surface coverage, and the value is in the range between 22 and 32 kcal/mole (*13–15*). However, Nishiyama and Wise (*13*) report 9 kcal/mole at high coverage, in agreement with our value of 8 kcal/mole. In an early work, Taylor *et al.* (*16*) reported a value of 12.2 kcal/mole for the heat of adsorption of CO on a

Pt black catalyst which was nearly saturated with CO. The base pressure for this experiment was approximately 1×10^{-5} Torr. By assuming the heat of adsorption is approximately equal to the activation energy for desorption, our value of 8 kcal/mole seems reasonable compared to the values reported in other studies.

4.2. *Surface Coverage of Adsorbed O and CO*

Comparison of the values in Column 1 and 3 in Table 1 indicate that the saturation coverages of oxygen and carbon monoxide are equal for all temperatures. These results are in good agreement with those of other investigators on Pt(111) oriented sheets (*12*) and single crystal surfaces (*5*). From the data in this experiment, we were not able to calculate the monolayer coverages of the adsorbed species. Nevertheless, the data allowed us to estimate the percentage of exposed Pt and the average particle size. Assuming that the ratio of CO/Pt_s is equal to 0.85(17), the percent of exposed Pt was calculated to be 6.8%. From this value, the particle size (assuming the particle were spherical) was estimated to be 166 Å. This value compares well with the average value from electron microscopy (200 Å).

4.3. *Surface CO during Transient Experiments*

4.3.1. Reaction of $O_2(g)$ with adsorbed CO. The dependence of the length of the induction period on flow rate and temperature can be explained by first examining the features involved in the adsorption of oxygen. The adsorption of oxygen is only possible if there are two adjacent free sites for dissociative adsorption (*11*). Therefore, when the catalyst surface is initially covered with carbon monoxide, at which time there are very few adjacent sites available for oxygen to adsorb dissociatively, adsorption of oxygen is inhibited. At 100–160°C, CO will desorb slowly from the surface in the absence of gas phase CO; thus eventually some sites for oxygen adsorption are created. Once oxygen adsorbs to the surface, it reacts with adsorbed CO to form CO_2. The number of available sites for oxygen to adsorb dissociatively will then increase as O_2 continues to adsorb and react with adsorbed CO. The rate of formation of CO_2, consequently, will be slow initially until a reasonable number of adjacent sites become available for oxygen to adsorb. After this time, the rate will increase rapidly.

The effect of temperature on the length of the induction time can be explained by the initial desorption experiments, in which we observed that the initial desorption rates of carbon monoxide increase with increasing temperatures. Consequently, the rate of evolution of sites which are available for oxygen adsorption also increases. This increase in the rate of desorption of CO results in the decrease in the induction times observed in Fig. 8.

The effect of flow rate on the induction time can be explained as follows: Carbon monoxide which is left in the reactor after $t = 0$ (the time at which the feed stream was switched from 2% CO to 3% O_2) is in equilibrium with the carbon monoxide adsorbed on the catalyst surface. The net desorption rate of adsorbed CO is dependent on the partial pressure of CO in the reactor which, in turn, is dependent on the residence time of the feed stream. When the flow rate to the reactor is decreased, the rate of removal of CO will decrease, and consequently, the induction time will be longer. From the results in Fig. 8, we observe this to be true with the exception of the flow rates greater than approximately 110 cm^3/min. Above 110 cm^3/min, the induction times were independent of flow rate. We refer to these induction times as the "absolute induction times." Figure 10 is a plot of the absolute induction time versus temperature. It appears that below 140°C, the effect of temperature on the induction times increases substantially. Similar results were reported by Bonzel and Ku (*5*) on a Pt(110) crystal.

The kinetics of these transient runs can

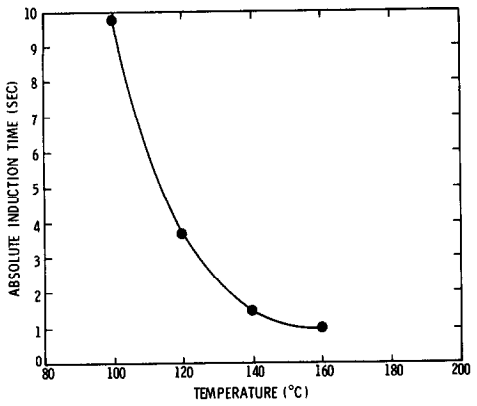

FIG. 10. The effect of temperature on the absolute induction time.

be interpreted in terms of a LH mechanism because of the observation of an induction period, indicating that $O_2(g)$ must adsorb before it can react.

4.3.2. Reaction of CO with adsorbed oxygen. The possible kinetic paths which are reported in the literature involving the reaction of CO with adsorbed O can be expressed as follows:

$$CO + P \longrightarrow CO \cdot P \xrightarrow{O_{ad}} CO_2 + * \quad \text{MER}$$

$$CO \cdot P \xrightarrow{*} CO_{ad} + O_{ad} \quad \text{LH}$$

where P represents a precursor site and * represents a chemisorption site. For both kinetic paths, the initial step is the incorporation of CO onto a precursor state. The paths then divide to one route following the modified Eley–Rideal (MER) process (*8*) in which CO·P reacts directly with O_{ad} to produce CO_2, and the other following the conventional Langmuir–Hinshelwood (LH) process in which carbon monoxide adsorbs first and then reacts with adsorbed oxygen (*11*).

From the results of our transient runs, we were able to conclude the following about the rates of the MER and LH processes relative to the rate of CO adsorption:

(1) The rate of the MER reaction is less than the rate of adsorption of CO because CO_2 is evolved at the same time the surface coverage of CO increases rapidly (Fig. 7). If the rate of the MER process were greater than the rate of CO adsorption, we would have observed the formation of CO_2 first and then the adsorption of CO.

(2) The rate of the LH reaction is less than the rate of adsorption of CO because of the initial rapid rate of CO adsorption (Fig. 6). If the LH process were faster than the adsorption rate of CO, the initial slopes of the transient curves in Fig. 6 would be considerably less.

(3) The rates of both the MER and LH combined are slower than the rate of adsorption of CO. The basis for this conclusion is obvious from the explanation of the first two.

In summary, the results indicate that the adsorption of CO is not the rate limiting step in the reaction of CO with adsorbed oxygen.

From the preceding discussion on the rates of the MER and LH processes relative to the rate of adsorption of CO, it is impossible to ascertain which mechanism predominates in the various regions of the transient curves shown in Fig. 6. However, if we assume that the rate of adsorption of CO indirectly measures the rate of CO_2 formation, the effect of temperature on the transient curves can provide information concerning the predominating reaction mechanism involved in the various regions of the curves. The results are now interpreted as follows: Because the initial portions of the transient curves are independent of temperature, indicating a low activation energy, we postulate that the MER process is initially the predominating mechanism. This assumption is further supported from the fact that CO_2 was produced immediately after CO entered the reactor. As the reaction proceeds, however, the LH process becomes the predominating reaction mechanism as noted by the temperature dependence of the transient curves.

Because the MER mechanism is merely a limiting case of the LH mechanism, it is

very difficult to state conclusively which mechanism predominates.

ACKNOWLEDGMENTS

This work was partly supported by NSF Grant ENG-7921890. We thank R. P. Eischens for the Pt/SiO_2 catalyst used.

REFERENCES

1. Bennett, C. O., *Catal. Rev. Sci. Eng.* **13**(2), 121–148 (1976).
2. Heyne, H., and Tomkins, F. C., *Proc. R. Soc. Ser. A.* **292,** 460 (1966).
3. Eischens, R. P., and Pliskin, W. A., *in* "Advances in Catalysis" (D. D. Eley, W. G. Frankenburg, and V. I. Komarewsky, Eds.), Vol. 10, pp. 2–54. Academic Press, New York, 1958.
4. Cutlip, M. B., *AIChE J.* **25**(3), 503–508 (1977).
5. Bonzel, H. P., and Ku, R., *Surf. Sci.* **33,** 91–106 (1972).
6. Cochran, H. D., Donnelly, R. G., Modell, M., and Baddour, R. F., *Colloid Interface Sci.* **3,** 131–142 (1976).
7. White, J. M., and Golchet, A., *J. Chem. Phys.* **61**(12), 5744–5747 (1977).
8. Matsushima, T., Almy, D. B., and White, J. R., *Surf. Sci.* **67,** 89–108 (1977).
9. Ueno, A., Hochmuth, J. K., and Bennett, C. O., *J. Catal.* **49,** 225 (1977).
10. Bennett, C. O., *ACS Symp. Ser.*, in press (1981).
11. Engel, T., and Ertl, G., *in* "Advances in Catalysis" (D. D. Eley, H. Pines, and P. B. Weisz, Eds.), Vol. 28, pp. 1–78. Academic Press, New York, 1979.
12. Ducros, R., and Merrill, R. P., *Surf. Sci.* **55,** 227–245 (1976).
13. Nishiyama, Y., and Wise, H., *J. Catal.* **32,** 50–62 (1974).
14. Collins, D. M., Lee, J. B., and Spicer, W. E., *Surf. Sci.* **55,** 384–402 (1976).
15. Winterbottom, W. L., *Surf. Sci.* **36**(1), 195–204 (1973).
16. Taylor, G. C., Kistiakowsky, G. B., and Perry, J. H., *J. Phys. Chem.* **34,** 799 (1930).
17. Freel, J., *J. Catal.* **25,** 149–160 (1972).